On the Single Bunch Emittance Preservation in TESLA

G.A. Amatuni, V. Khachatryan, V.M. Tsakanov
Yerevan Physics Institute
R. Brinkmann
Deutsches Elektronen-Synchrotron

1 Introduction

The main aspects of the single bunch emittance preservation in the TESLA main linac are discussed in this report. The wakefield and dispersive emittance dilution of the beam in the case of a coherent betatron oscillation and the misalignment of an accelerating section or quadrupole/BPM has been studied. The corresponding correction technique has been applied to keep the emittance dilution of the beam at the level of a few percent. The study includes the two-beam operation part of the linac, where the beams for High Energy physics (HEP) and X-Ray Free Electron Laser(FEL) are accelerated in an interleaved pulse mode.

2 Linear Optics and Cell Arrangement

After the damping ring and bunch compressor, the electron beam for high energy physics is injected into the main linac at the energy of 5 GeV and is accelerated up to the energy of 250 GeV with an acceleration gradient of 23.4 MV/m . The main parameters of the injected beams are given in Table 1.

Table 1: Parameters of the HEP and FEL beams.

Parameters	TESLA	FEL
Energy $E[GeV]$	5	2.5
Charge per bunch $Q[nC]$	3.2	1
Bunch RMS length $\sigma_z[mm]$	0.3	0.025
Initial uncorrelated RMS energy spread $\sigma_\in$	2.5%	0.1%
Norm. emittance hor./vert. at inj. $\varepsilon_{x,y}[mm \cdot mrad]$	8/ 0.02	0.7
Norm. emittance hor./vert. at e^+e^- IP $\varepsilon_{x,y}[mm \cdot mrad]$	10/ 0.03	-

The linac is divided in two sections, with quadrupole spacings of 4 and 6 cryo-modules, respectively (Fig.1). The change of FODO cell arrangement is located at the middle of linac when the beam has reached an energy of 125 GeV.

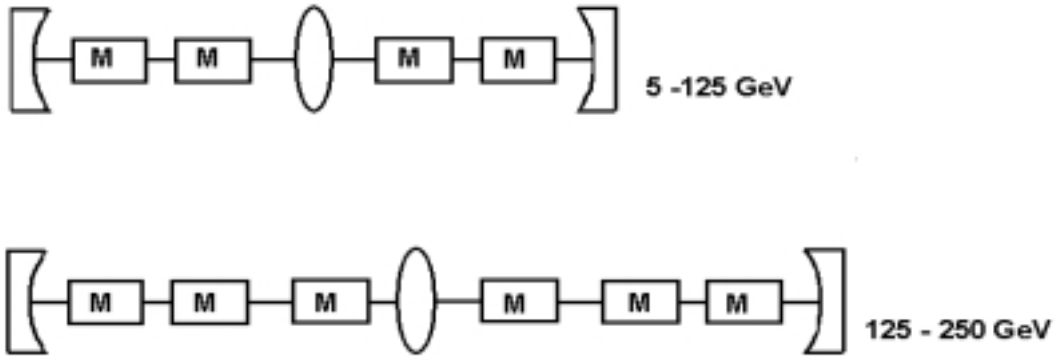

Fig.1 *Quadrupole spacing (in unit of cryomodules) for TESLA.*

The main parameters of the TESLA focusing lattice are given in Table 2.

TABLE 2. Parameters of TESLA focusing lattice.

Quadrupole, effective length [m]	0.6
Quadrupole, geometrical length [m]	0.9
Cell length 5-125 GeV [m]	65
Phase advance per cell μ_T	45^o,60^o
Cell length 125-250 GeV [m]	96.6
Phase advance per cell 125-250 μ_T	60^o
Maximum gradient of quadrupoles at 400 GeV [T/m]	47

The specific aspect of the TESLA design is that the low energy part of the main linac (first ≈3 km, 5-55 GeV) will be used to accelerate the beam for the X-Ray Free Electron Laser facility and HEP beam in an interleaved pulse mode. In the first section of the linac, which is used for the FEL and the HEP beams, the 60^o-lattice (HEP) is also suitable for the FEL beam over most of its foreseen energy range. At low FEL energy operation (corresponding to an accelerating gradient of 9.2 MV/m), a reduction to 45^o per cell for the high energy beam is necessary to avoid over-focusing of the low-energy FEL beam, which sees a phase advance per cell of about 120^o.

Simultaneous operation of two very different energy beams in a linac which follows the curvature of the earth leads to intolerable systematic dispersive orbit offsets [2]. To avoid the effect, this section of the linac is chosen to align along an exact straight line (in contrast to previous layout [1]). To enable the option for producing collisions of protons stored in HERA with electrons from the main linac, there is a transition from the initial slope of the HERA ring into the

horizontal direction of the TESLA electron beam at the angle about 8 mrad. The transition to the line following the earth's curvature is provided by an achromat bend insertion directly after the high-energy FEL beam extraction point.

2.1 Low energy two-beam operation.

The injection energy of the beams into the TESLA main linac for HEP and FEL operation modes are E_T=5 GeV and E_F=2.5 GeV. The optical solution for the FEL beam in thin lens approximation is given by

$$\sin[\mu_F(n)/2] = \sin(\mu_T/2)\frac{E_T(n)}{E_F(n)} \tag{1}$$

where $\mu(n)$ is the phase advance in n-th FODO cell, $E(n) = E_0 + U \cdot (n-1)$ is the energy at the entrance of the n-th cell, U is the energy gain per FODO cell, and the subscript (T, F) indicates the HEP and FEL options respectively.

To provide a maximum energy range for the FEL beam with a minimum number of extraction points, the betatron phase advance per FODO cell for the HEP beam is chosen to be μ_T =45 degree for the lowest acceleration gradient of FEL beam 9.2 MV/m. An energy range of the FEL beam of 13-47 GeV is provided by two extraction points from the main linac.

The acceleration gradient for the FEL operation can in principle lie between 9.2 and 23.4 MV/m, where an optical solution for the FEL beam exists. However, at present FEL operation is only foreseen up to 35 GeV beam energy and typically the accelerating gradient will be in the range 9.2 to 17 MV/m.

The first extraction point covers the energy range of 13-27 GeV, and the second extraction point covers the range of 20-47 GeV. Due to the overlap of energy ranges, both beamlines may be operated in the same energy range of 20-27 GeV, if desired.

Tables 3 presents the main parameters of the beam at the extraction points from the main linac.

Table 3. Parameters of Extraction Points

Extraction ports	Port 1	Port 2
Energy range $E_F[GeV]$	13...27	20...47
Acceleration gradient $G_F[MV/m]$	10...23.4	9.2...23.4
Number of FODO cells	21	38
Position along the linac $L_1[m]$	1365	2470
Phase advance in last FODO cell μ	$120^o - 47^o$	$125^o - 45^o$

The phase advance per cell along the linac for the FEL beam with different acceleration gradients is presented in figure 2. The 22-th and 39-th FODO cells are used for the extraction magnets.

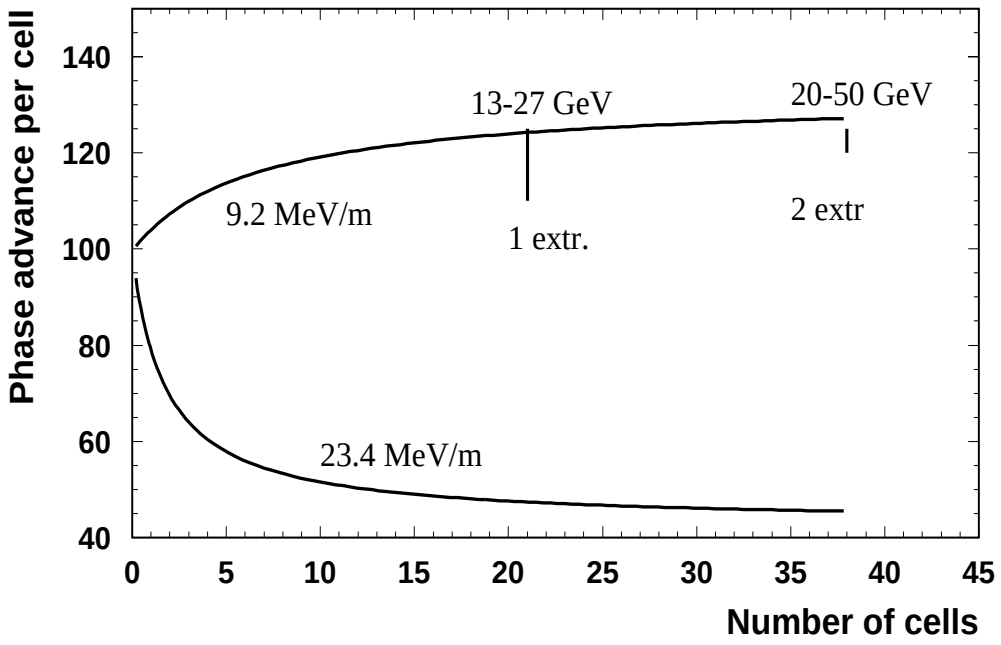

Fig.2 *The phase advance per cell of the FEL beam along the main linac for different operation energies.*

2.2 The achromatic bending section.

The Linear Collider will be built underground at a depth of about 15 m. The interaction point HERA west is about 20 m above sea level. The axis of the main part of the linac tunnel lies about 10 m below sea level. The straight section HERA West has a slope of about 8 mrad out of the horizontal plane. Therefore, to enable the option for producing collisions of protons stored in HERA with electrons from the main linac, there is a transition from the initial slope into the horizontal direction of the electron beam. Fig.3 shows a vertical profile of the linear collider area North-Northwest of DESY together with the collider tunnel. The low energy part of the linac is straight to avoid any effect due to dispersion. In contrast to the previous solution (ref. [1], indicated by the 915 km bending radius in Fig. 3), the transition from the initial slope into the horizontal direction is now provided by a local bend of the 55 GeV TESLA beam in an achromat section after the extraction of the FEL beam.

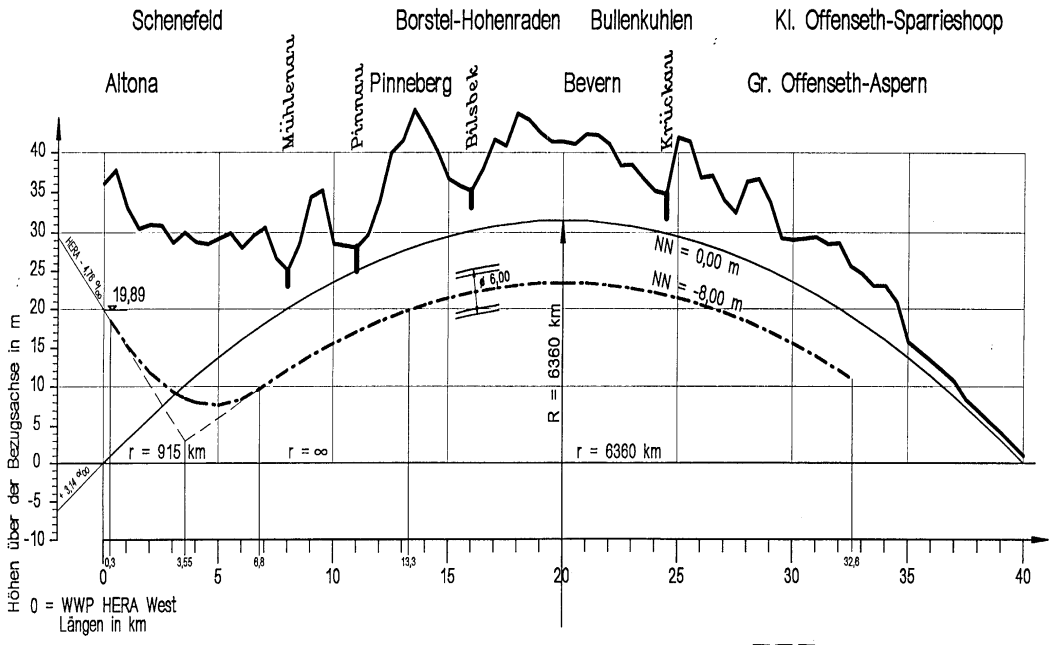

Fig.3 *Vertical profile of the Linear Collider area North-Northwest of DESY.*

The minimum bending radius of the TESLA beam is defined by the emittance growth of a 200 GeV electron beam (the electron-proton collision option with a 250 GeV electron beam) caused by incoherent synchrotron radiation. In a transport line, the emittance growth ($\Delta\varepsilon/\varepsilon << 1$) due to incoherent synchrotron radiation can be estimated by [3]

$$\Delta(\gamma\varepsilon)[m \cdot rad] \approx 4.13 \cdot 10^{-8} E^6[GeV] I_5[m^{-1}], \qquad (2)$$

where E is the beam energy in GeV and I_5 is the fifth synchrotron integral. The maximum emittance growth of the 200 GeV beam is estimated to be at the level of $\Delta(\gamma\varepsilon) \approx 10^{-7} m \cdot rad$. The optimization of the achromat cell optics is based on the minimization of fifth synchrotron integral. The betatron and dispersion functions of the transition transport line is shown in Fig. 4. The two bending magnets BY and the quadrupoles QF provide the achromatic vertical bend of the 55 GeV TESLA beam by an angle of 8 mrad. The length of the bending magnet is 10 m with a magnetic field of 72 mT. The two end quadrupole doublets (Q1,Q2) provide the matching of the optical functions and allowed to obtain the optimal beam envelope along the transport line. The quadrupole strengths that provide a complete matching of the twiss parameters are given in Table 4. The fifth synchrotron integral of the transport line is equal to $I_5 = 2.6 \cdot 10^{-14} m^{-1}$. An expected emittance dilution of a 200 GeV due to incoherent synchrotron radiation is then at the level of $\Delta(\gamma\varepsilon) \approx 0.7 \cdot 10^{-7} m \cdot rad$.

TABLE 4. Parameters of achromatic bending section.

Quadrupole length $[m]$	0.6
Strength Q1/Q2/QF $[m^{-2}]$	0.2/-0.2/0.25
Maximum gradient $[T/m)$	57
Dipole length $[m]$	10
Dipole field $[mT]$	72
Maximum dispersion $[mm]$	27
Total length $[m]$	41.5

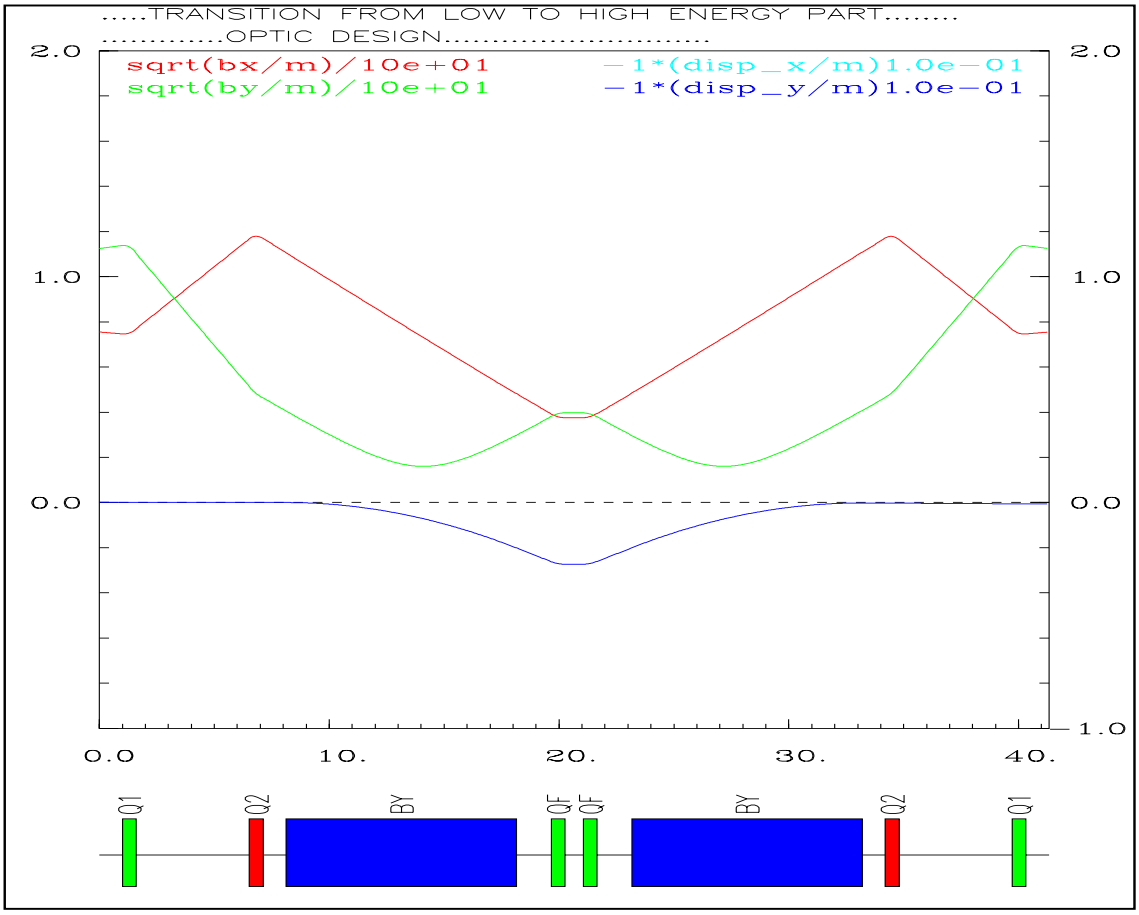

Fig.4 *The betatron and dispersion functions in achromat matching section*

3 The wake potentials and energy spread

When a short bunch travels through the accelerator, it gains energy from externally driven accelerating mode and loses energy due to the longitudinal wakefields. The net energy deviation of the particle at the position s within the bunch and position z along the linac is then given by

$$\Delta E(z,s) = eQzW_z(s) + \hat{G}z\cos(\phi_{RF} + \frac{2\pi}{\lambda_{RF}}s) - Gz = U(s)z, \tag{3}$$

where W_z is the longitudinal wake potential per unit length, $\hat{G}$, G are the maximum and the average accelerating gradient, Q is the total charge of the bunch, ϕ_{RF}, λ_{RF} are the accelerating phase and the wavelength of the RF system.

The wake potential of a charge distribution is given by the convolution of the point charge wake potential with the charge distribution

$$W_z(s) = \frac{1}{Q}\int_{-\infty}^{s} \rho(s)w(s-s')ds', \tag{4}$$

The analytical expression for a point wake potential is used to approximate the wake function. The longitudinal point charge wake function of TESLA averaged per unit cavity length is given by [4]

$$w(s) = 38\left[\frac{V}{pCm}\right]\left(1.165\cdot\exp\left(-\sqrt{\frac{s}{3.65mm}}\right) - 0.165\right) \tag{5}$$

Fig. 5 presents the longitudinal wake potential for the HEP and the FEL beams in the TESLA cavity. The relative correlated energy spread induced in an accelerating sections varies with the energy as

$$\epsilon_{cor}(s,z) = \frac{\Delta E(s,z)}{E(z)} = \frac{U(s)}{G}\left[1 - \frac{\gamma_0}{\gamma(z)}\right], \tag{6}$$

where $\gamma_0, \gamma(z)$ are the initial and actual Lorentz factors of the design particle. The rms value of the parameter $\delta(s) = U(s)/G$ is determined by the longitudinal impedance of accelerating structure, amplitude, frequency and RF phase of accelerating mode, the length and total charge of the bunch.

Fig. 6 presents the rms energy spread of the HEP and FEL beams induced in the main linac versus the RF phase of the accelerating mode. The optimal phase for the HEP beam is $\phi_{RF} = 5.3$ degree for TESLA-500 (acceleration gradient 23.4 MV/m). It is reasonable to accelerate the FEL beam at the RF sinusoidal wave crest $\phi_{RF} = 0$. Different FEL beam energies can be achieved by a variation of the RF amplitude of the accelerating mode.

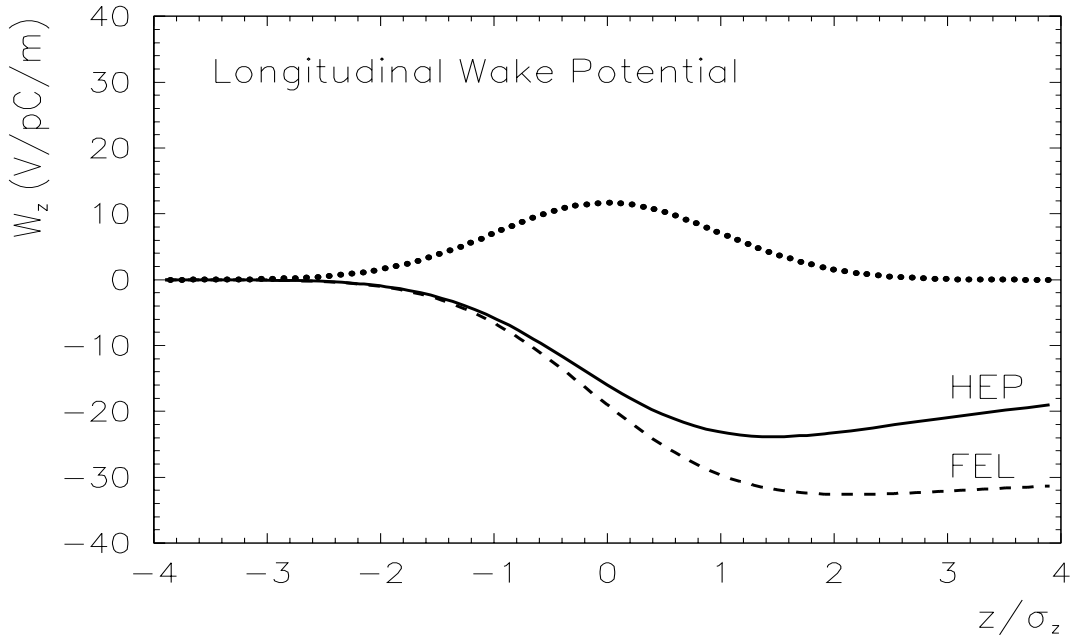

Fig.5 *Longitudinal monopole wake potentials for HEP (solid line) and FEL (dashed line) beams.*

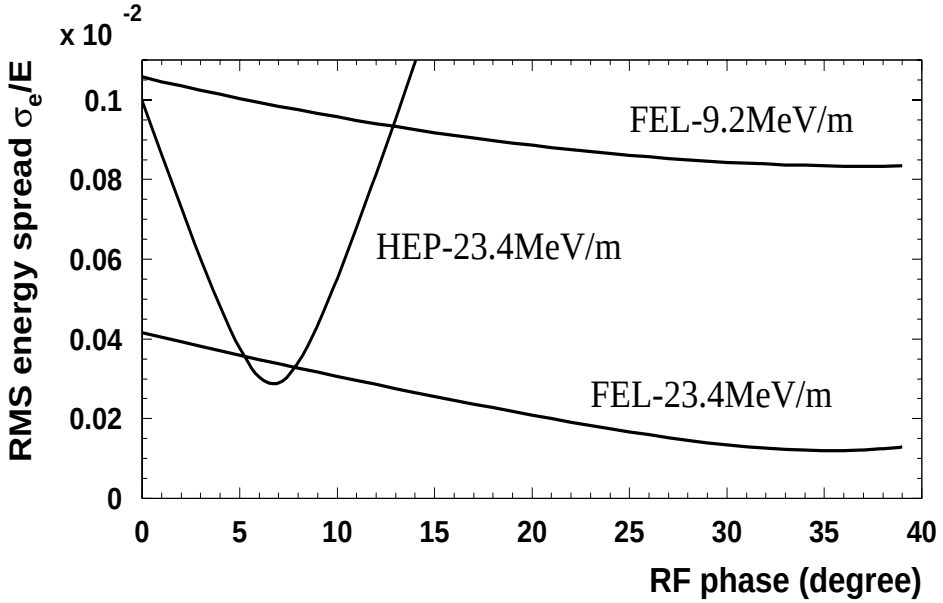

Fig.6 *The RMS energy spread for the HEP and the FEL beam versus the accelerating RF phase.*

An off-axis beam in cylindrically symmetrical accelerating structure produces transverse wake fields which act back on the trailing particles. The short range

dipole transverse wake potential of a point charge is used for single bunch instability calculations. The short range dipole transverse wake potential of a point charge for the TESLA cavity is given in Ref. [5] by the fitting of the transverse impulse factor

$$w_x = \frac{1}{L_{cav}}(1290\sqrt{\frac{s}{m}} - 2600\frac{s}{m}) \ \ [V/pC/m^2] \tag{7}$$

where s is the position with respect to the exciting point-like charge. The dipole wake potentials of the HEP and FEL beams are shown in Fig. 7.

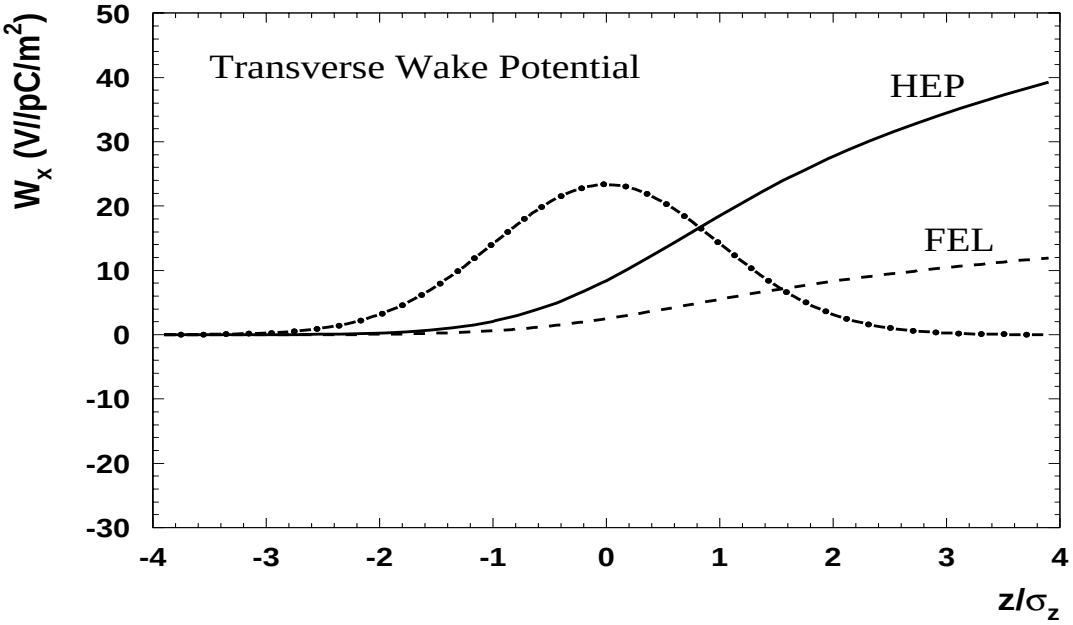

Fig.7 *Dipole transverse wake potentials for HEP (solid line) and FEL (dashed line) beams.*

The value of the point transverse dipole wake potential at the distance 2σ is equal to : 28.98 $V/pC/m^2$ for the HEP beam and 8.68 $V/pC/m^2$ for the FEL beam.

4 Free Coherent Oscillation

One of the unwanted features of the linear accelerators is an uncontrolled injection jitter which lead to coherent betatron oscillation of the beam. We consider the case when the beam is entering the main linac with initial amplitudes (y_0, y_0'). The main effects, which accompany the coherent oscillating beam, are the beam filamentation in the focusing lattice due to the initial uncorrelated energy spread (dispersive effects) and the transverse deflection of the trailing particles by wakefields induced by off-axis motion of the beam (wakefield effects). In addition, the longitudinal wakefield and the interaction of the beam with Radio-Frequency (RF) accelerating field induces a correlated energy spread leading to a correlated dispersive effect that can dominate or reduce the transverse wakefield effects.

4.1 Dispersive effects

Usually the beam that is entering to the main linear accelerator of the collider has an uncorrelated energy spread due to processes in the bunch compressor or damping ring. If the chromaticity of the focusing lattice does not vanish the off-energy particles acquire the betatron phase shift that is being accumulated along the linac. The bunch starts to filament: a particle with higher energy oscillates with lower frequency, while a particle with lower energy oscillates with higher frequency with respect to a design particle.

For the initial Gaussian energy distribution, the emittance dilution averaged over the actual phase $\mu(z)$ is given by

$$\frac{\Delta\varepsilon}{\varepsilon}(z) = \frac{1}{2}\frac{a_0^2}{\varepsilon_0}\left[1 - \exp\left(-\Delta\mu_s^2(z)\right)\right] \tag{8}$$

where ε_0 is the initial natural emittance of the beam, $\Delta\mu_s$ is the betatron phase shift of off-energy particle with rms energy spread $\sigma_{\epsilon 0}$ and

$$a_0^2 = \gamma y_0^2 + 2\alpha y_0 y_0' + y_0'^2 \tag{9}$$

Formula (6) indicates that the maximum dispersive relative emittance dilution for one sigma initial offset ($a_0^2 = \varepsilon_0$) is limited by 0.5 that corresponds to the case when the diluted beam occupies the annular region of the machine ellipse. This is usually the case for high chromaticity lattices.

For lower chromaticity beam optics like in TESLA, where $\Delta\mu_s/2\pi << 1$, the formula can be written as (for one sigma offset):

$$\frac{\Delta\varepsilon}{\varepsilon} = \frac{1}{2}\Delta\mu_s^2 = 2\sigma_{\epsilon 0}^2 \tan^2(\mu/2)\left(\frac{\gamma_0}{\Delta\gamma}\right)^2 \ln^2\frac{\gamma(z)}{\gamma_0} \tag{10}$$

where $\Delta\gamma$ is the energy gain per FODO cell. The emittance dilution of the HEP beam in TESLA is shown in Fig. 8. It amounts to about 6.5% for a one

sigma oscillation (here and in the following, the emittance growth for the collider beam is always quoted relative to the vertical design emittance at the IP, see Table 1). We expect to control the injection into the linac to better than 10μm, corresponding to half a beam sigma, which will result in an emittance growth below 2%.

The emittance dilution of the FEL beam for different acceleration gradients is shown in Fig. 9.

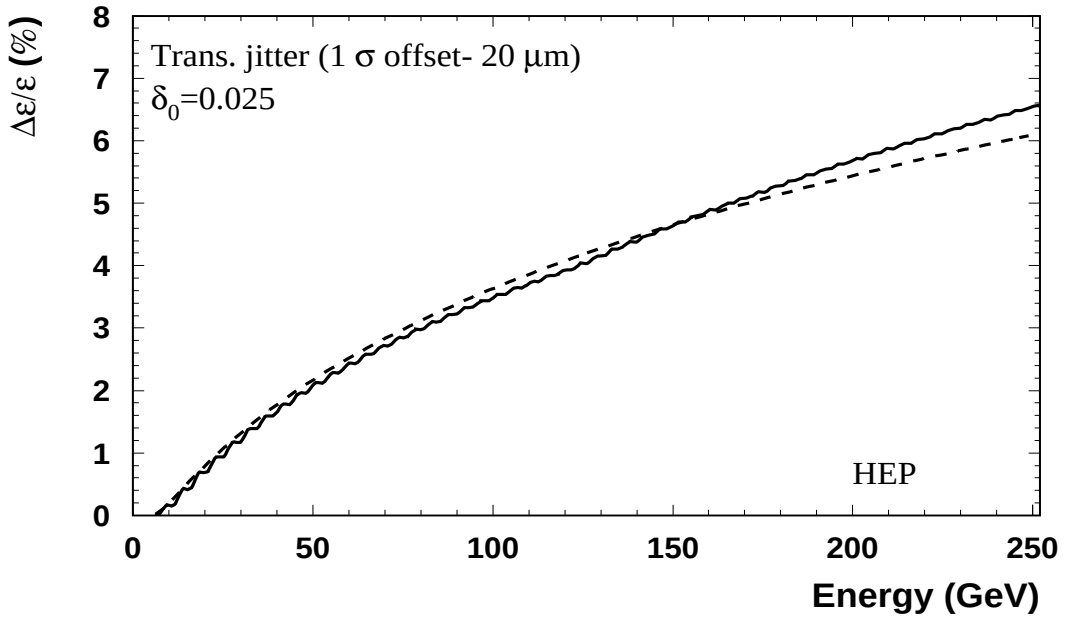

Fig. 8 *Dispersive emittance dilution of the HEP beam caused by an injection offset and an initial uncorrelated energy spread. The solid line shows the particle tracking simulation, and the dashed line the analytical prediction for a constant beta FODO lattice.*

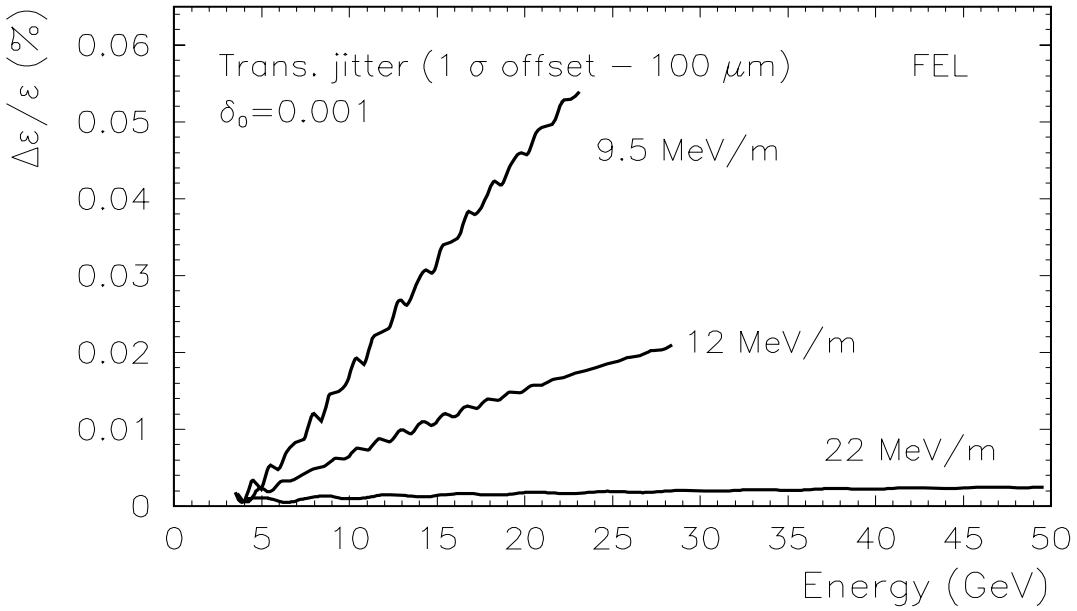

Fig. 9 *Dispersive emittance dilution of the FEL beam caused by an injection offset and an initial uncorrelated energy spread for different acceleration gradients.*

4.2 Wakefield effects

An interaction of the beam with the accelerating structure leads to an induced correlated energy spread due to longitudinal wakefields and the external RF accelerating field, and a deformation of the transverse shape of the bunch due to transverse wakefields for an off-axis beam.

The dispersive emittance dilution due to a correlated energy spread is given by

$$\frac{\Delta\varepsilon}{\varepsilon} = \frac{1}{2}\frac{a_0^2}{\varepsilon_0}\left(1 - \frac{\sin^2\Delta\hat{\mu}}{\Delta\hat{\mu}^2}\right), \tag{11}$$

where $\Delta\hat{\mu}$ is the phase shift of the particle with maximum energy deviation $\hat{\epsilon} = \sqrt{3}\delta_{rms}$. Again the emittance dilution is limited by 0.5 for an offset of one standard deviation, and a beating of the off-energy slices around the machine phase ellipse is observe for a high dispersive machine. For a low dispersive machine, we obtain the following emittance dilution

$$\frac{\Delta\varepsilon}{\varepsilon} = \frac{1}{6}\frac{a_0^2}{\varepsilon_0}\Delta\hat{\mu}^2 = 2\frac{a_0^2}{\varepsilon_0}\left[\delta_{rms}\frac{\gamma_0}{\Delta\gamma}\tan\frac{\mu}{2}\left(\frac{\gamma}{\gamma_0} - \ln\frac{\gamma}{\gamma_0} - 1\right)\right]^2, \tag{12}$$

where δ_{rms} is the energy spread due to longitudinal wakefields and the RF accelerating mode. By proper choice of the accelerating RF phase ($\phi_{RF} = 5.3^o$) one can provide a small correlated energy spread in the bunch. In addition, the small

transverse wake fields in TESLA allow to increase the number of accelerating modules per single FODO cell and to reduce the betatron phase advance per cell. All this provide a low chromaticity of the machine and results in a very small dispersive emittance dilution of the beam. The dispersive emittance dilution for the HEP beam is shown in Fig 10.

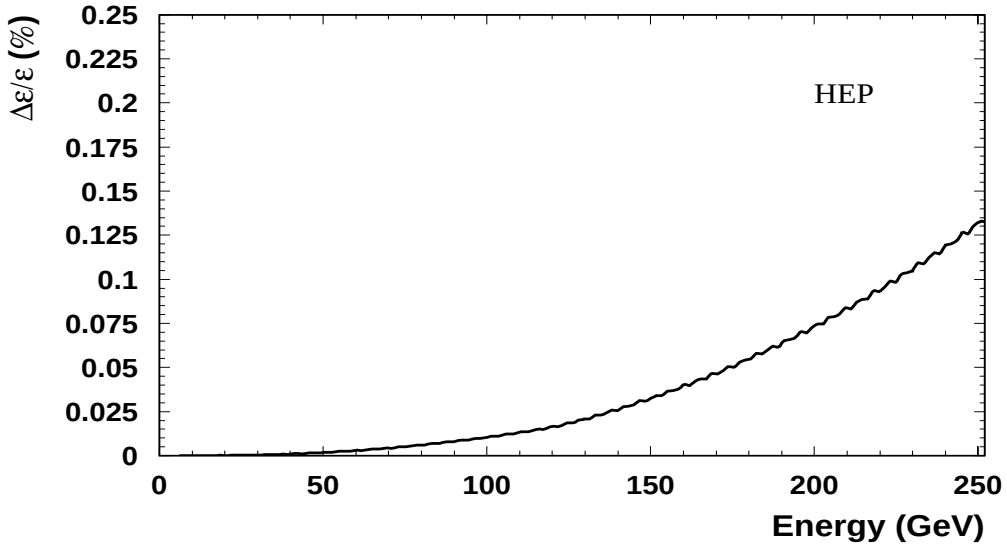

Fig. 10 *Dispersive emittance dilution caused by a correlated wakefield induced energy spread.*

The emittance enlargement of the bunch by transverse wake fields in a constant beta lattice machine is given by [6]

$$\frac{\Delta\varepsilon}{\varepsilon}(z) = \frac{1}{2}\frac{a_0^2}{\varepsilon_0}\left(\frac{eQW_dL_c}{8G}\right)^2 \frac{1}{\sin^2\mu}\ln^2\frac{\gamma(z)}{\gamma_0}, \tag{13}$$

where L_c is the focusing cell length, G is the acceleration gradient. Fig.11 and 12 show the emittance dilution of the HEP and the FEL beams due to transverse wakefields. The tracking simulations include the correlated energy spread induced in the accelerating sections due to the accelerating RF mode and the longitudinal wakefields.

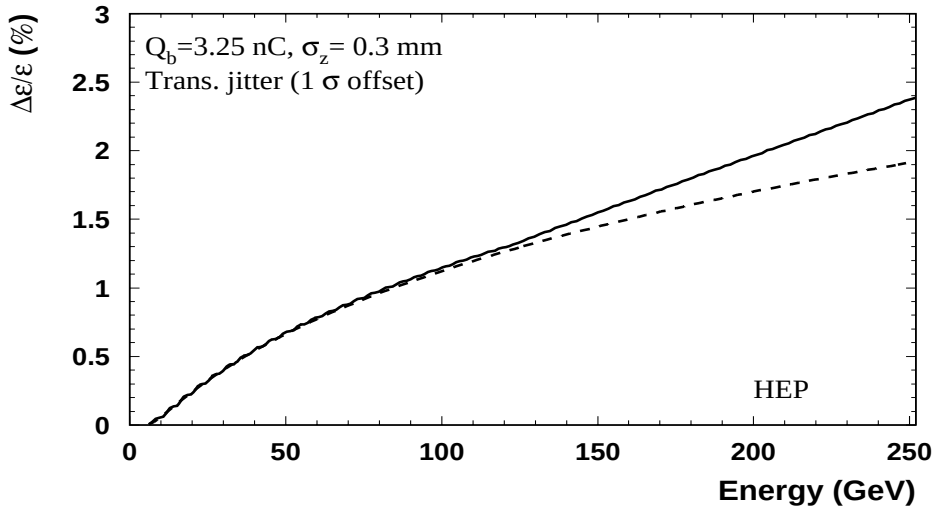

Fig.11 *Emittance dilution of the HEP beam caused by transverse wakefields. The solid line shows the tracking simulation, and the dashed line the analytical prediction.*

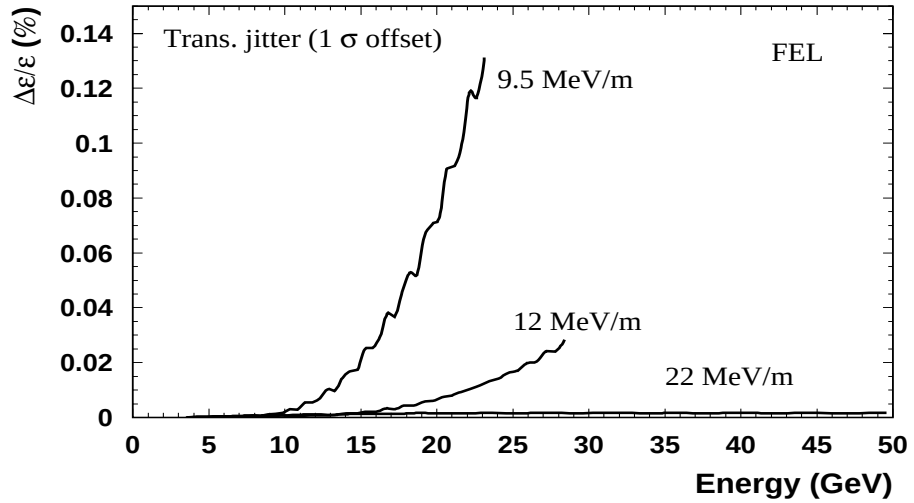

Fig.12 *Emittance dilution of the FEL beam caused by transverse wakefields for different accelerating gradients.*

5 Cavity misalignments

Consider the linear accelerator with misaligned cavities. The beam is traversing the accelerating sections with nonzero offset with respect to cavity axis and thus excite the transverse wakefields which enlarge the beam transverse emittance.

The rms emittance dilution calculated in a two particle model is given by

$$\frac{\Delta\varepsilon(z)}{\varepsilon} = \frac{< y_a^2 >}{2N_{cav}\varepsilon_0}\left(\frac{eQW_D}{4G}\right)^2 \frac{\Delta\gamma}{\gamma_0}\frac{L_{cell}}{\sin\mu}\ln\frac{\gamma(z)}{\gamma_0} \tag{14}$$

where N_{cav} is the number of the cavities per single FODO cell. Fig. 13 presents the emittance dilution of the TESLA HEP beam averaged over 50 random sets for cavity misalignment with an rms value $\sigma_{cav} = 0.5\ mm$. The rms emittance dilution at the end of linac is at the level of 7%.

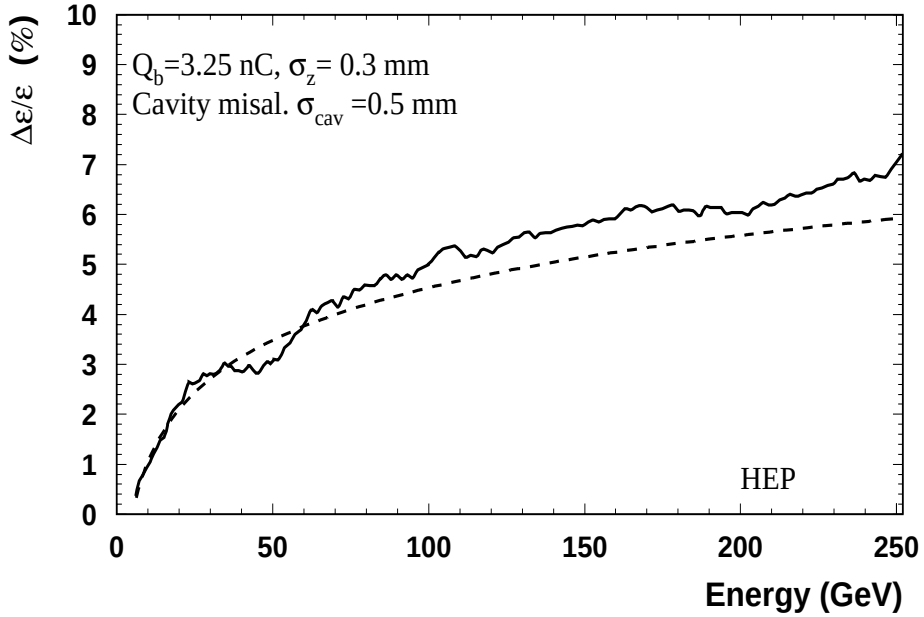

Fig. 13 *Rms emittance dilution of the HEP beam due to the cavity misalignment ($\sigma_{cav} = 0.5\ mm$). The dashed line is an analytical prediction ($\mu = 45$ degree).*

The emittance dilution of the FEL beam by wakefields is presented in Fig. 14 for different operation gradients. The maximum emittance dilution is for low operation gradient and is below 10^{-4}.

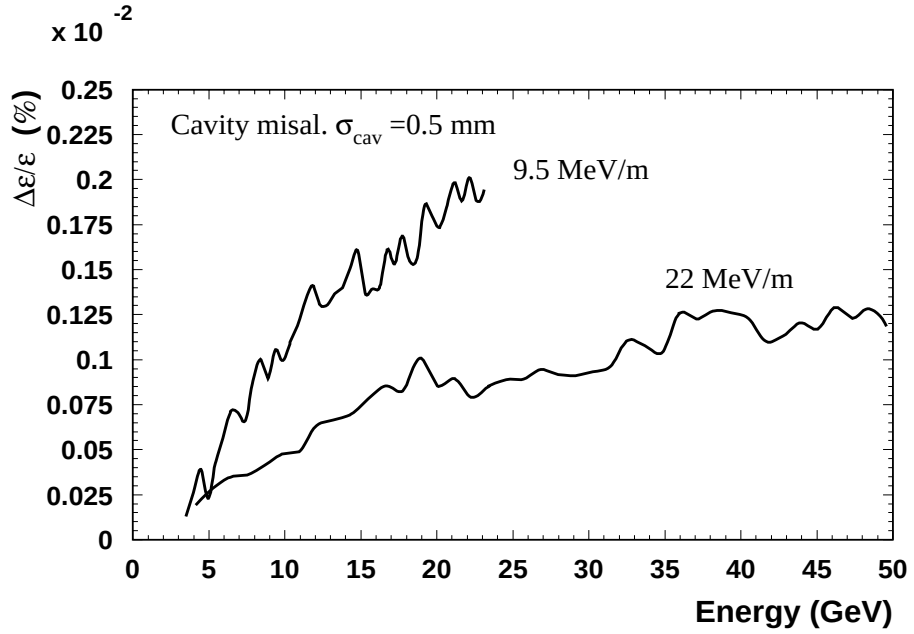

Fig. 14 *Rms emittance dilution of the FEL beam due to the cavity misalignments* ($\sigma_{cav} = 0.5mm$).

Fig. 15 shows the emittance enlargement probability function calculated for 2000 random seeds for the linac with uniform random cavity misalignment with an rms cavity offset $\sigma_{cav} = 0.5mm$.

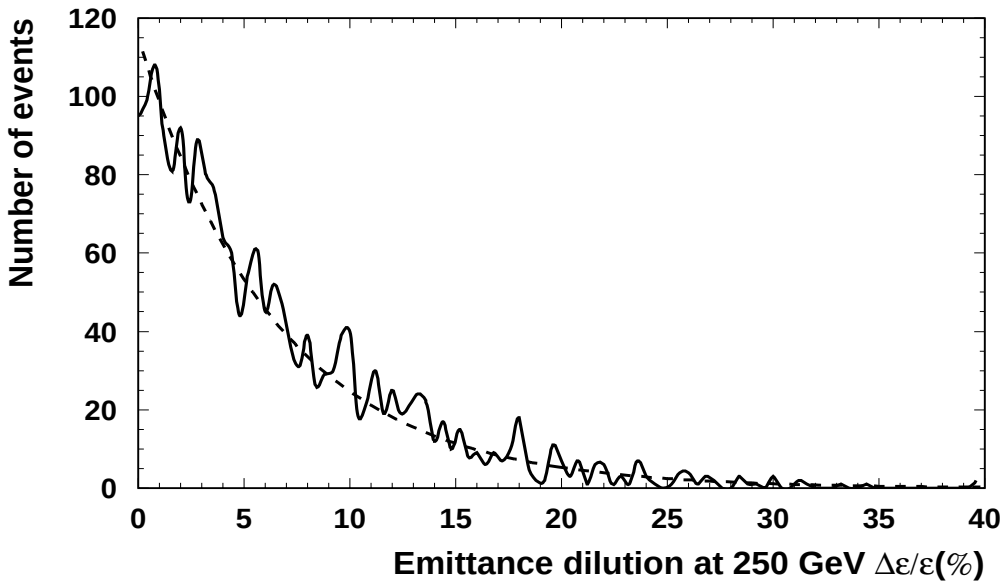

Fig. 15 *The probability of the rms emittance dilution of the HEP beam due to the cavity misalignment* ($\sigma_{cav} = 0.5mm$, *2000 random seeds*).

The distribution has a pronounced character of a exponential distribution. The empirical approximation of the probability distribution for 2000 uniform

random seeds is given by

$$N(\epsilon) = N(0) \exp\left(-\frac{\xi}{<\xi>}\right) \tag{15}$$

where $\xi = \Delta\varepsilon/\varepsilon$, and $<\xi>$ is the average emittance dilution of the beam over N number of seeds.

The correction procedure to reduce the emittance enlargement due to the cavity misalignment is based on the idea of using the beam trajectory to correct the wakefield dilutions. The correction schemes envision a manipulation of the beam trajectory with simultaneous measurement of the beam emittance. The beam trajectory is deflected by the non-dispersive bump and at some location downstream of the bump the emittance is measured and the magnitude of the bump adjusted until the emittance reaches a minimum. An individual Non-Dispersive (ND) bump extends over 5 quadrupoles/dipole sets, starting at a focusing quadrupole.

The simulation results show that an optimal bump for the correction is a single bump with opposite polarities located at the position of 57 and 151 GeV (Fig.16). The emittance is measured at the end of the linac in the beam delivery system.

Fig. 17 shows the reduction of the emittance enlargement with adjusted bumps for one random seed of cavity misalignments.

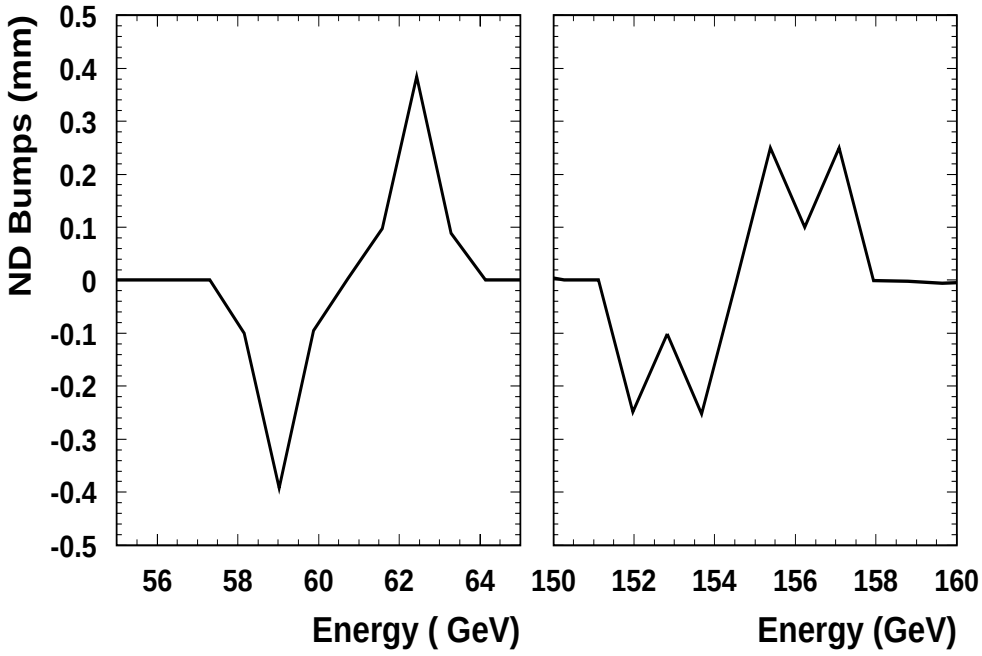

Fig. 16 *The ND bumps for TESLA*

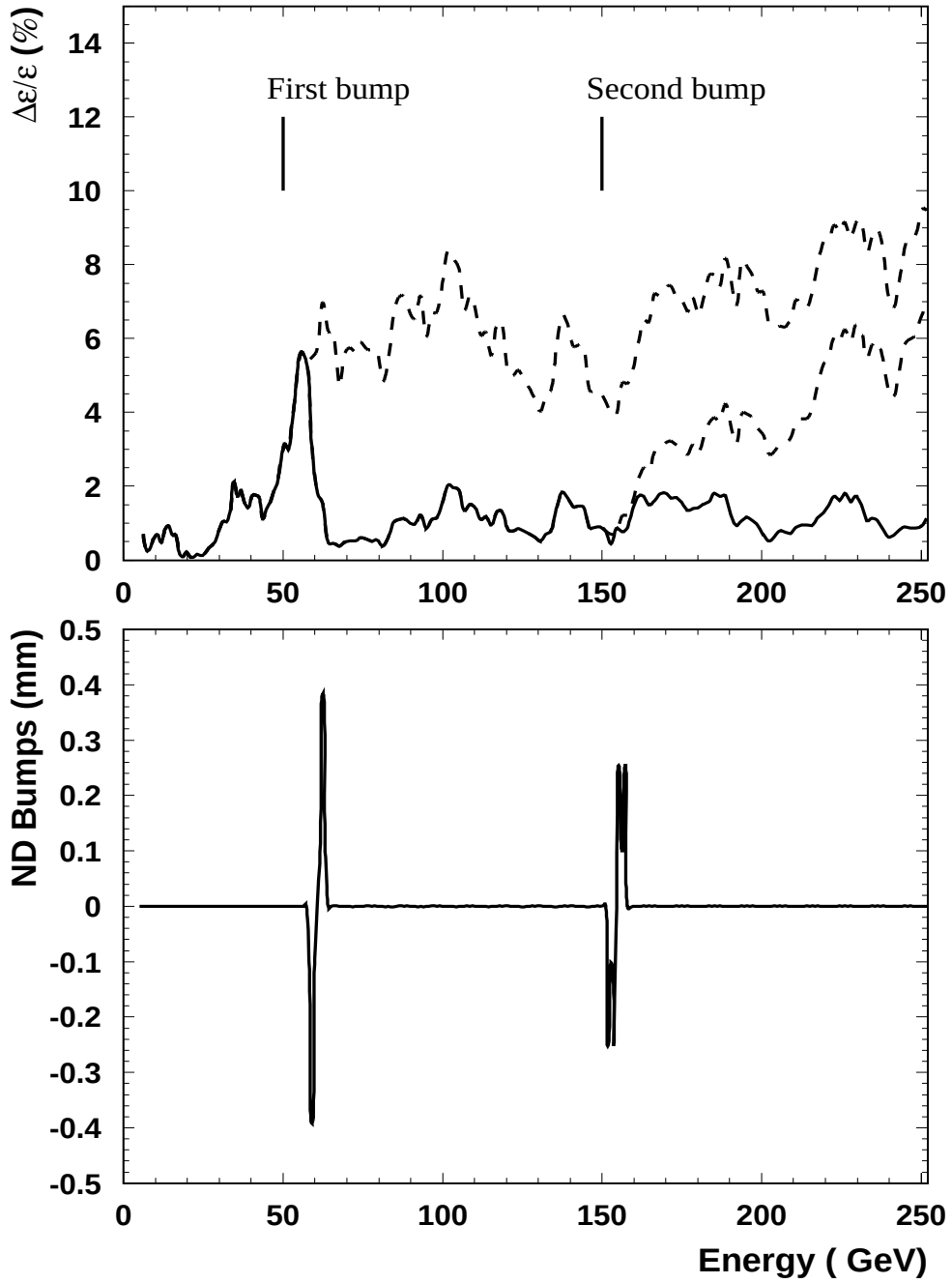

Fig. 17 *The ND Bumps and the reduction of the emittance dilution by cavity misalignment.*($\sigma_{cav} = 0.5mm$). *The upper figure shows the emittance growth without bumps (upper dashed line), with one bump (lower dashed line) and with two bumps (full line).*

6 One-to-one correction

We assume that the trajectory is corrected to the quadrupole centerline in each F and D quadrupole using Beam Position Monitor (BPM) measurements. The quadrupoles are randomly misaligned with the rms value σ_q, the BPMs are randomly misaligned with respect to the quadrupole center with the rms value σ_b. In addition, the BPMs have a resolution with the rms expected value σ_r. After performing a one-to-one correction (minimization of the BPM measurements), the beam central trajectory $y_c(z)$ in the quadrupoles is given by $y_{ck} = q_k + b_k + r_k$, where q_k, b_k,and r_k are uncorrelated random values of quadrupole and BPM misalignments, and the BPM resolution .

The rms uncorrelated dispersive emittance dilution in a thin lens approximation is given by

$$\frac{\Delta\varepsilon}{\varepsilon} = 8\delta_{0rms}^2 \frac{< y_c^2 >}{\varepsilon_0 L_c} \frac{\gamma_0}{\Delta\gamma} \tan\frac{\mu}{2} \cdot \ln\frac{\gamma(z)}{\gamma_0}, \tag{16}$$

where δ_{0rms} is the initial uncorrelated energy spread of the beam, $\Delta\gamma$ is the energy gain per cell in terms of Lorentz factor. To predict the emittance dilution caused by the wakefields, we assume that the off-axis trajectory of the beam in the accelerating sections is given by $y_{ac} = (y_F + y_D)/2$ with the rms expected value $< y_{ac}^2 >=< y_c^2 >$. The predicted rms emittance dilution is then given by

$$\frac{\Delta\varepsilon(z)}{\varepsilon} = \frac{< y_c^2 >}{4\varepsilon_0} \left(\frac{eQW_D}{4G}\right)^2 \frac{\Delta\gamma}{\gamma_0} \frac{L_c}{\sin\mu} \ln\frac{\gamma(z)}{\gamma_0} \tag{17}$$

Fig. 18 shows the rms dispersive and wakefield emittance dilution for a TESLA beam, when the trajectory is corrected by a one-to-one correction technique. The rms value of the misalignment are

Quadrupole misalignments $\sigma_q = 0.3\,\mathrm{mm}$
BPM misalignments..... $\sigma_b = 0.1\,\mathrm{mm}$
BPM resolution..... $\sigma_r = 10\,\mu\mathrm{m}$

The simulation results are averaged over 50 random seeds for the misalignment. The dispersive emittance dilution for TESLA is very large. In addition, it is well understood that in the two beam operation mode with large energy difference, the FEL beam performs large coherent betatron oscillations when the trajectory of the HEP beam is corrected by the one-to-one correction method [2].

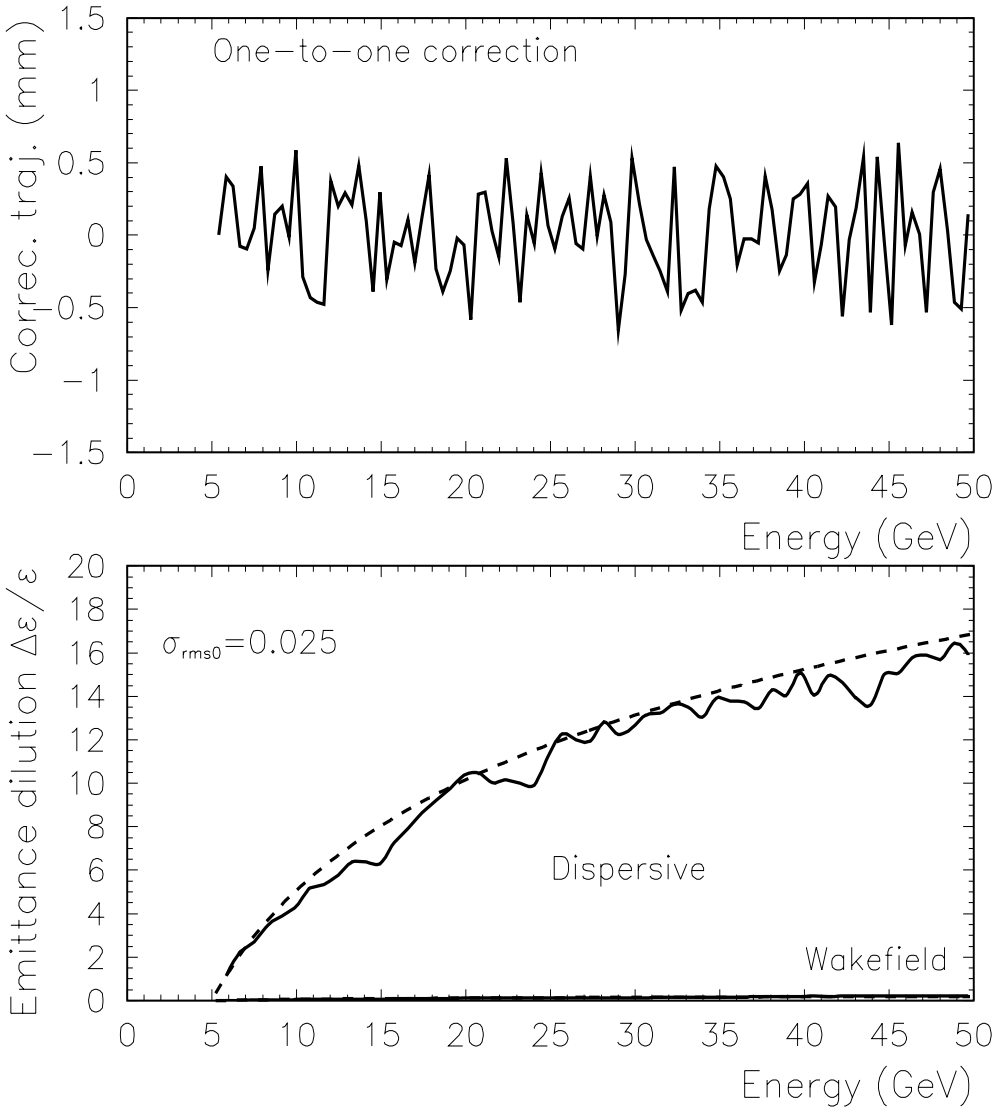

Fig. 18 *The one-to-one corrected trajectory of the HEP beam in the TESLA main linac (top) and the rms dispersive and wakefield emittance dilution of the beam* ($\sigma_q = 300\mu m, \sigma_b = 100\mu m, \sigma_r = 10\mu m$). *The dashed line is the analytical prediction.*

7 Beam-based trajectory correction

The TESLA design with the integrated FEL beam opens the possibility to use the information on the trajectories from two beams with different energies to minimize the difference orbit by fitting the strength of the corrector dipoles. The procedure is essentially similar to the dispersion free trajectory correction algorithm [8]. But we apply it for two beams with a large relative energy difference.

We assume, that the quadrupoles are misaligned with respect to a ideal straight line through the linac.

To correct the difference orbit of the HEP and FEL beams with different energies E_T, E_F, we need to measure the beam trajectories. If we only consider transverse deflections due to quadrupole misalignments and dipole correctors, the k-th BPM will measure

$$m_{Tk} = r_k(t_1) + b_k + \sum_{l=1}^{k-1} \theta_l M_{12}^t(z_l, z_k), \tag{18}$$

$$m_{Fk} = r_k(t_2) + b_k + \sum_{l=1}^{k-1} \frac{E_{Tk}}{E_{Fk}} \theta_l M_{12}^f(z_l, z_k) \tag{19}$$

where θ is the integrated deflection of the dipole correctors and the quadrupole misalignments, $r_k(t_1), r_k(t_2)$ are the BPM resolutions for two independent measurements for HEP and FEL beams, z is the position of the BPMs along the linac. The difference orbit is then independent of the BPM misalignments and is given by

$$\Delta m_k = [r_k(t_2) - r_k(t_1)] + \sum_{l=1}^{k-1} \theta_l \left[M_{12}^t(z_l, z_k) - \frac{E_{Tk}}{E_{Fk}} M_{12}^f(z_l, z_k) \right] \tag{20}$$

where $M_{12}^{t,f}$ is the transport matrix element for the HEP (t) and the FEL (f) beams. Then, in principal, we could solve the equation for the N_q unknown quadrupole misalignment, assuming that the BPM precision errors and any unknown deflections are negligible. Including the BPM precision errors, the amplitude of the difference orbit could be reduced at the level of the BPM precision errors. However, the minimization of the difference orbit amplitude does still not provide a reduction of the amplitude of the real trajectories at the level of BPM precision errors. The real trajectories diverge from the linac centerline and the rms amplitudes of the trajectories of the HEP and FEL beams grow with the quadrupole number. This occurs because the difference orbit is not referenced to the linac centerline and small errors add up along the linac. Thus we have to include some information about the absolute trajectory while correcting the difference orbit.

The two trajectory corrections algorithm for TESLA has been studied numerically for two cases: first based on the BPM readings of one passage of the HEP and FEL beam over the 43 FODO cells, and second using a multi-stage trajectory correction. A least square fit for the unknown dipole corrector strengths has been performed, using the original HEP trajectory *and* the difference orbit weighted with the absolute accuracy with which these trajectories are known [7, 8]:

$$\sum_k \frac{(m_{Tk} + y_{Tk})^2}{\sigma_r^2 + \sigma_b^2} + \frac{(\Delta m_k + \Delta y_k)^2}{2\sigma_r^2} \tag{21}$$

Fig. 19 (top) shows the corrected HEP and FEL beam trajectories using a dispersion free procedure over the first 43 FODO cells. The actual energies of the HEP beam and the FEL beam are related as 5/3 (the acceleration gradient of the HEP beam is 23 MV/m, and 14 MV/m for the FEL beam). To reduce the diffusion of the trajectories a multistage correction has been applied.

The procedure of the multi-stage correction is as following: After a dispersion free correction over the first 20 FODO cell based on BPM reading of the HEP and FEL trajectories, the values of the corrector dipoles in first 5 FODO cell are fixed. The next stage is an application of dispersion free correction for the next 20 cell (cells 6-25) which is based on the new BPM readings. Again, the values of the corrector dipoles in next 5 FODO cells (FODO cells 6-10) are fixed. The next step of the procedure is performed over the cells 11-31 based on new BPM readings. The total number of steps for 43 FODO cell is 8. The errors still add, but the resulting amplitudes of the trajectories are now at the level about 40-50 μm at the end of the low energy part of the linac (Fig.21, bottom figure).

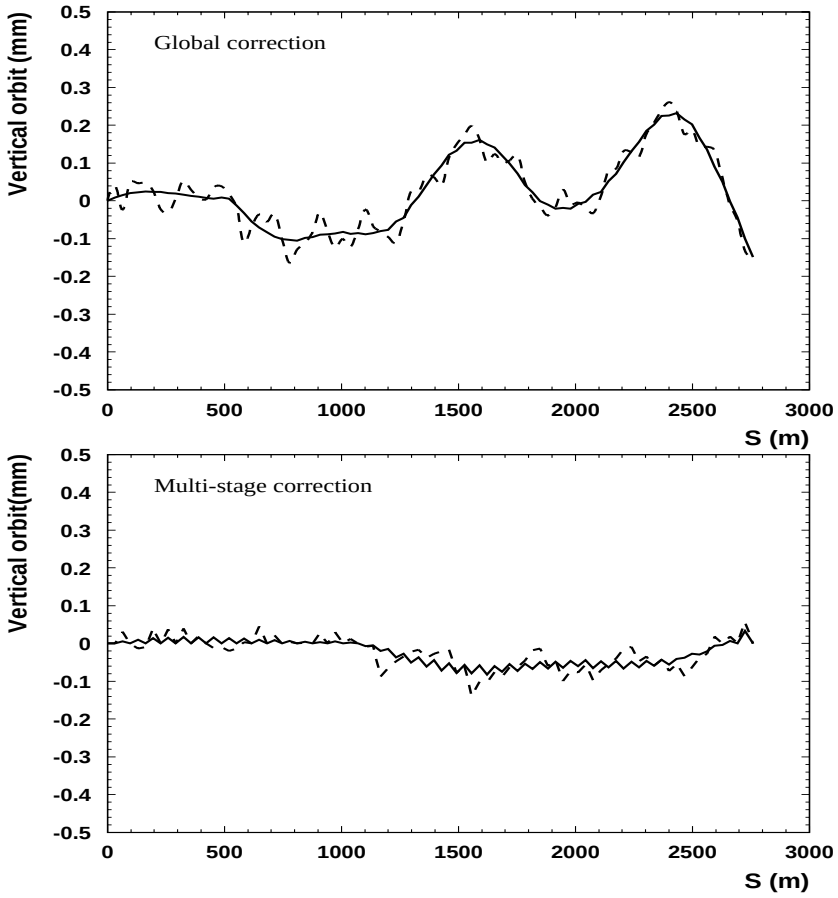

Fig. 19 *Two beam based trajectory correction for TESLA. The trajectories of the HEP beam (solid line) and the FEL beam are shown after a global correction (top) and after performing a multi-stage correction (bottom).* ($\sigma_q = 0.3mm, \sigma_b = 0.1mm, \sigma_r = 10\mu m$)

The dispersive (uncorrelated) and wakefield (correlated) emittance dilutions of the HEP beam is shown in Fig. 20 after performing a multi-stage two beam based trajectory correction.

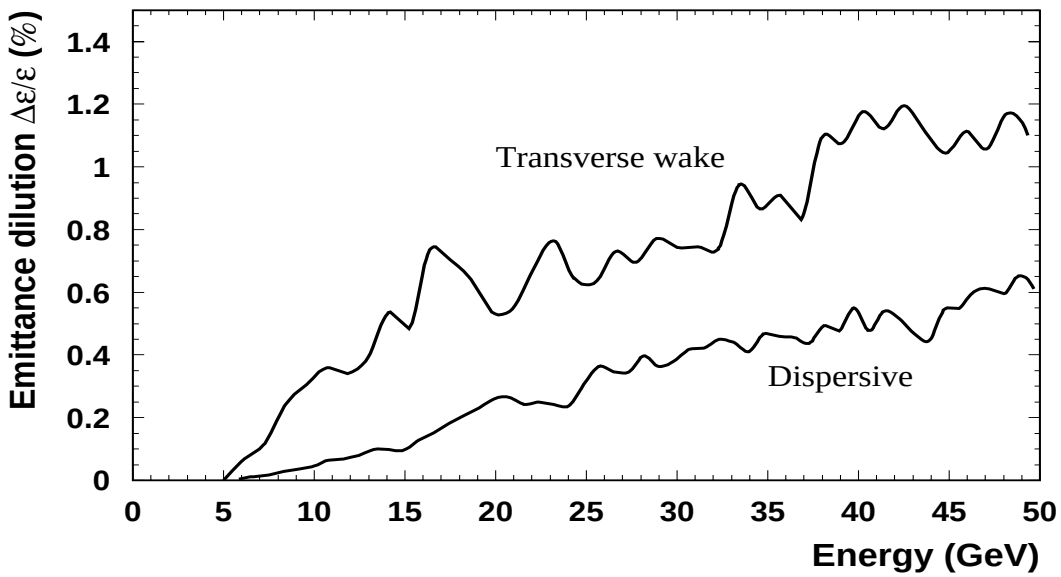

Fig.20 *Correlated(transverse wakefield) and uncorrelated (dispersive) emittance dilution of HEP beam in the first section of the main linac after the application of a two-beam based multi-stage trajectory correction.*

Thus, the application of a multistage two beam based trajectory correction with given quadrupole and BPM misalignment of TESLA allows the stabilization of the trajectory correction of both beams (HEP and FEL) beams at the level of BPM misalignment with a drift after 40 FODO cells at the level of 40 μm. The dispersive and wakefield emittance dilution is at the level of 1% for HEP beam and at the level of 10^{-4} for FEL beam.

The multi-stage correction procedure has been applied for HEP beam along the entire linac. The results from computer simulations are shown in Fig. 21. The BPMs measure the trajectories of HEP beam at two energies E_1 and E_2, that are related as 5/3. The corresponding operation gradients for the HEP beam are 23.4 MV/m and 16 MV/m (in practice, changing the strengths of all magnets by this ratio instead of the beam energy may be the easier way). The total number of steps to correct the trajectory along the entire linac is 40. The resulting drift of the orbit at the end of the linac is at the level of 100-150 μm. The dispersive emittance growth obtained by averaging over 50 random seeds of misalignment amounts to 1% for an iterative procedure, in which the DF-algorithm is applied to sections of 20 FODO cell per step. The residual orbit deviations after the DF-correction yield an additional emittance growth due to transverse wakefield of 2% (Fig.21).

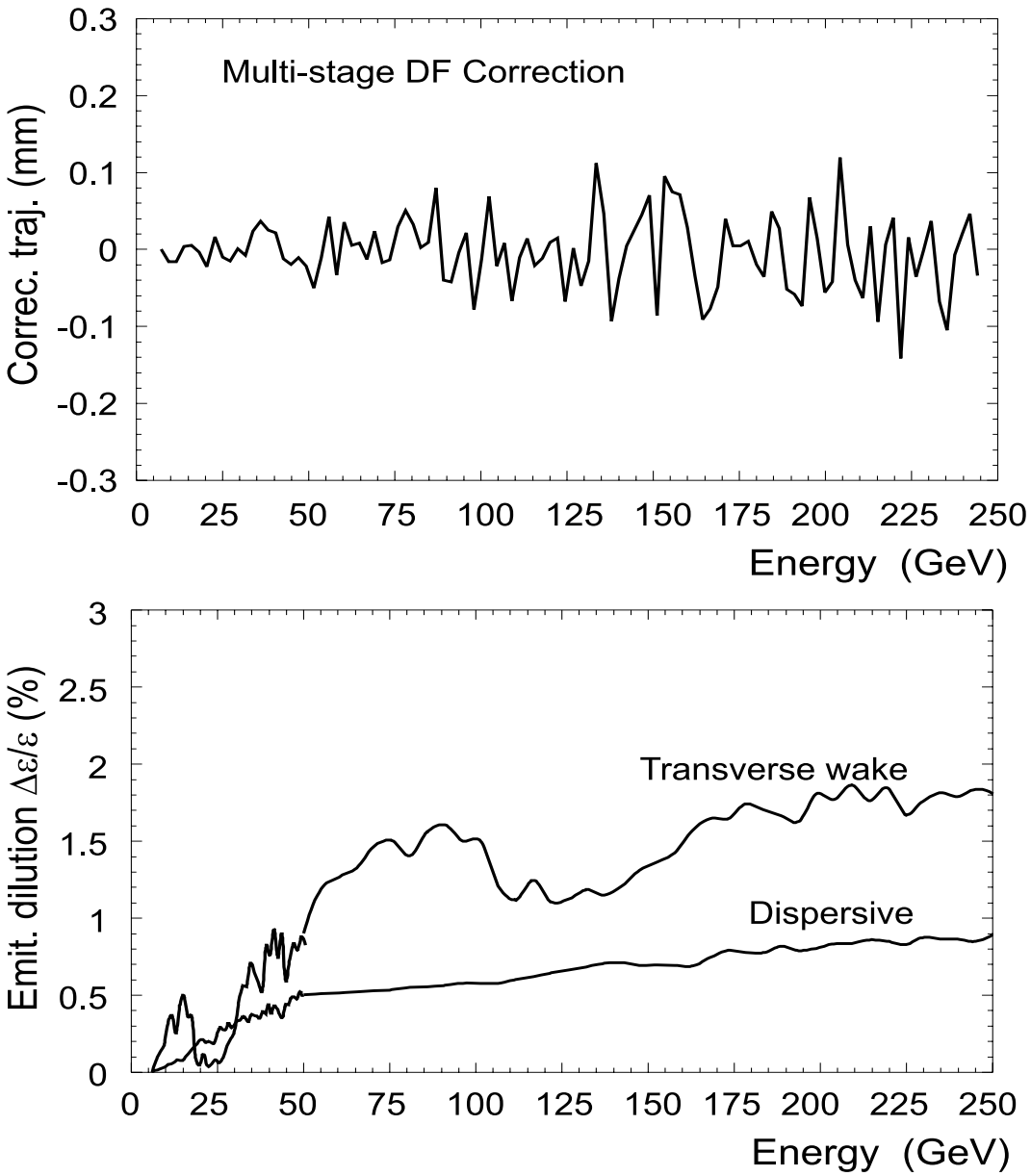

Fig. 21 *Beam orbit (top) and emittance dilution (bottom) along the entire linac after a multi-stage dispersion free correction.*

For the trajectory correction of the HEP beam in the entire linac it is reasonable to apply the multi-stage DF correction of the orbit up to the an energy of 125 GeV. For high energy part of the linac (125-250 GeV) the one-to-one trajectory correction procedure already provides a negligible wakefield caused emittance dilution, and a residual uncorrelated emittance dilution at the level of 3.5%.

Summary

The main aspects of the emittance preservation in the TESLA main linac, including the correction algorithm, have been studied. It has been shown, that the emittance dilution from cavity misalignments is below 10% and by application of well established corrections techniques, like non-dispersive bumps for cavity misalignment, can be further reduced to the level of 1-2%. Injection errors which we expect to have a typical amplitude of one half of the beam size lead to additional emittance growth of the same order of magnitude. A special study has been performed for application of the dispersion free correction algorithm for the linac with misaligned quadrupoles. A multi-stage DF correction algorithm has been developed to minimize the deviation of the absolute beam trajectories from the linac centerline. An application of the multi-stage algorithm for the entire linac resulted in a correlated (transverse wake) emittance dilution of the beam of 2% and in a uncorrelated (dispersive) one of about 1%.

Acknowledgments

The authors would like to express their thanks to Rainer Wanzenberg for carefully reading the manuscript and for very useful comments.

References

[1] *Conceptual Design of a 500 GeV e^+e^- Linear Collider with Integrated X-Ray Laser Facility*, edited by R. Brinkmann, G. Materlik, J. Rossbach and A. Wagner, Hamburg, DESY 1997-048, 1997.

[2] V.M. Tsakanov, Beam Dynamics Study for TESLA with the Integrated FEL, DESY TESLA-99-21, 1999.

[3] M. Sands, Emittance Growth from Radiation Fluctuations, SLAC-AP-47 , 1985.

[4] A. Novokhatsky, M. Timm, Th. Weiland, Single Bunch Energy Spread in the TESLA Cryomodule, DESY TESLA-99-16, 1999.

[5] A.Mosnier, Longitudinal and Transverse Wakes for the TESLA, DESY TESLA-93-11,1993.

[6] K.Bane, SLAC-PUB-4169,1986.

[7] C.E. Adolphsen etc, SLAC-PUB-4902, March 1989.

[8] T.O. Raubenheimer and R.D. Ruth, NIM (A), **302**, 191 (1991).